Supplementary Information

Synthesis, band structure and photocatalytic property of Sillén–Aurivillius oxychlorides $BaBi_5Ti_3O_{14}Cl$, $Ba_2Bi_5Ti_4O_{17}Cl$ and $Ba_3Bi_5Ti_5O_{20}Cl$ with triple-, quadruple- and quintuple-perovskite layers

Daichi Ozaki,[ab] Hajime Suzuki,[a] Kanta Ogawa,[ab] Ryota Sakamoto,[a] Yoshiyuki Inaguma,[c] Kouichi Nakashima,[d] Osamu Tomita,[a] Hiroshi Kageyama*[a] and Ryu Abe*[ab]

[a]*Department of Energy and Hydrocarbon Chemistry, Graduate School of Engineering, Katsura, Kyoto University, Nishikyo-ku, Kyoto 615-8510, Japan*
[b]*AIST-Kyoto University Chemical Energy Materials Open Innovation Laboratory (ChEM-OIL), National Institute of Advanced Industrial Science and Technology (AIST), Yoshida, Sakyo-ku, Kyoto 606-8501, Japan*
[c]*Department of Chemistry, Faculty of Science, Gakushuin University, Toshima-ku, Tokyo 171-8588, Japan*
[d]*Department of Materials Science and Engineering, Graduate School of Science and Engineering, Ibaraki University, 4-12-1, Nakanarusawa, Hitachi, Ibaraki 316-8511, Japan*

Corresponding Authors
*kage@scl.kyoto-u.ac.jp (H.K.); ryu-abe@scl.kyoto-u.ac.jp (R.A.)

This supporting information presents the following contents.

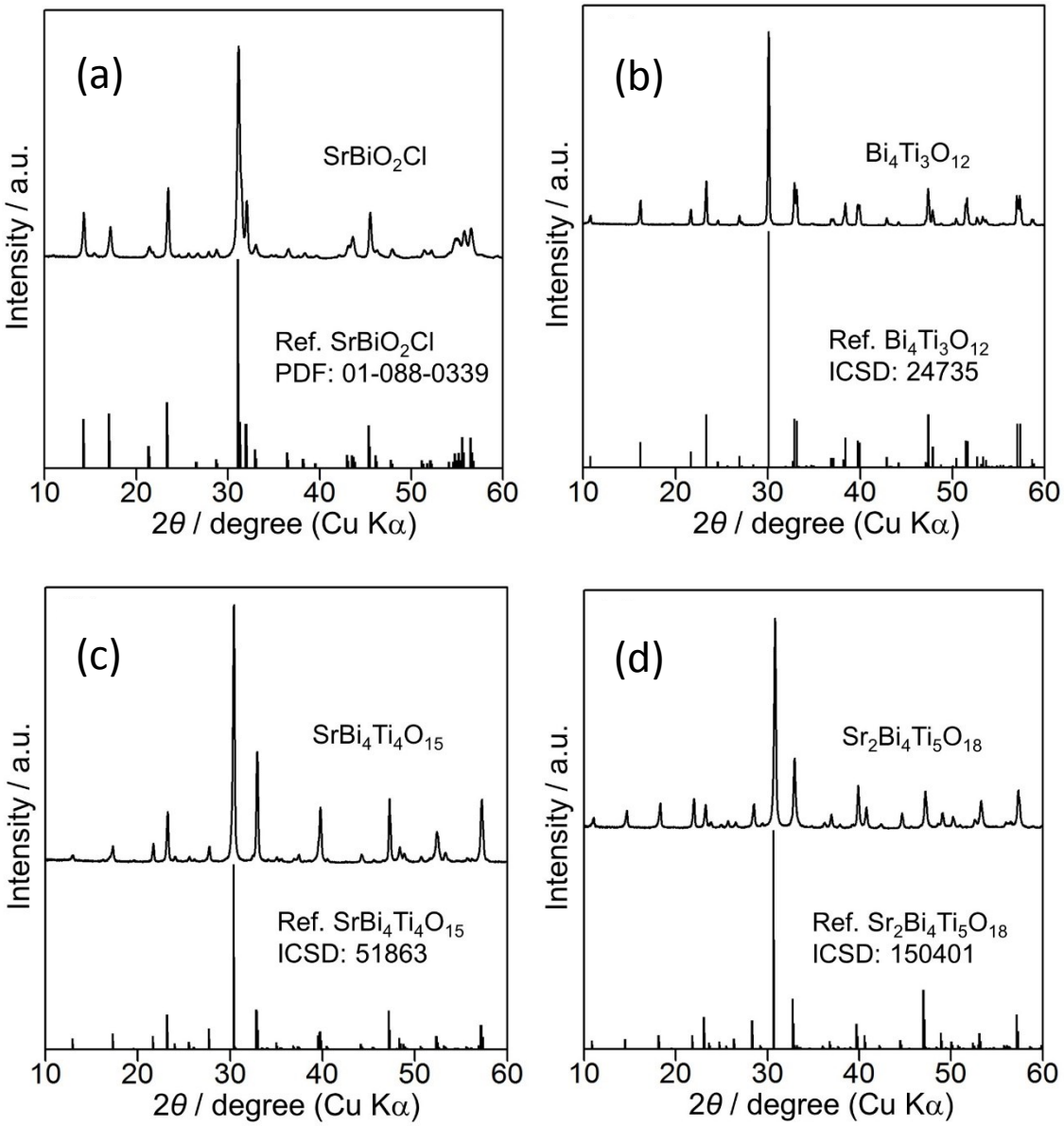

Fig. S1 XRD patterns of (a) $SrBiO_2Cl$, (b) $Bi_4Ti_3O_{12}$, (c) $SrBi_4Ti_4O_{15}$ and (d) $Sr_2Bi_4Ti_5O_{18}$.

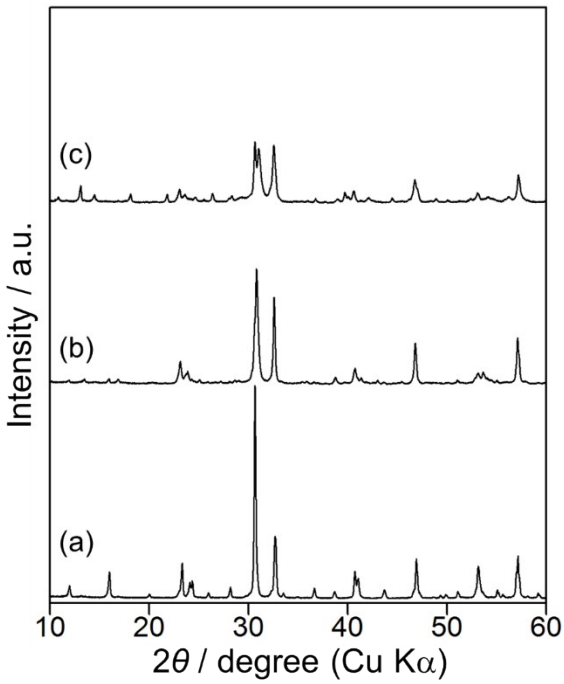

Fig. S2 Laboratory XRD patterns of Sr-containing Sillén–Aurivillius compounds. (a) $Bi_5SrTi_3O_{14}Cl$ (n = 3), (b) $Bi_5Sr_2Ti_4O_{17}Cl$ (n = 4) and (c) $Bi_5Sr_3Ti_5O_{20}Cl$ (n = 5). Note that (b) and (c) are not fully crystallized.

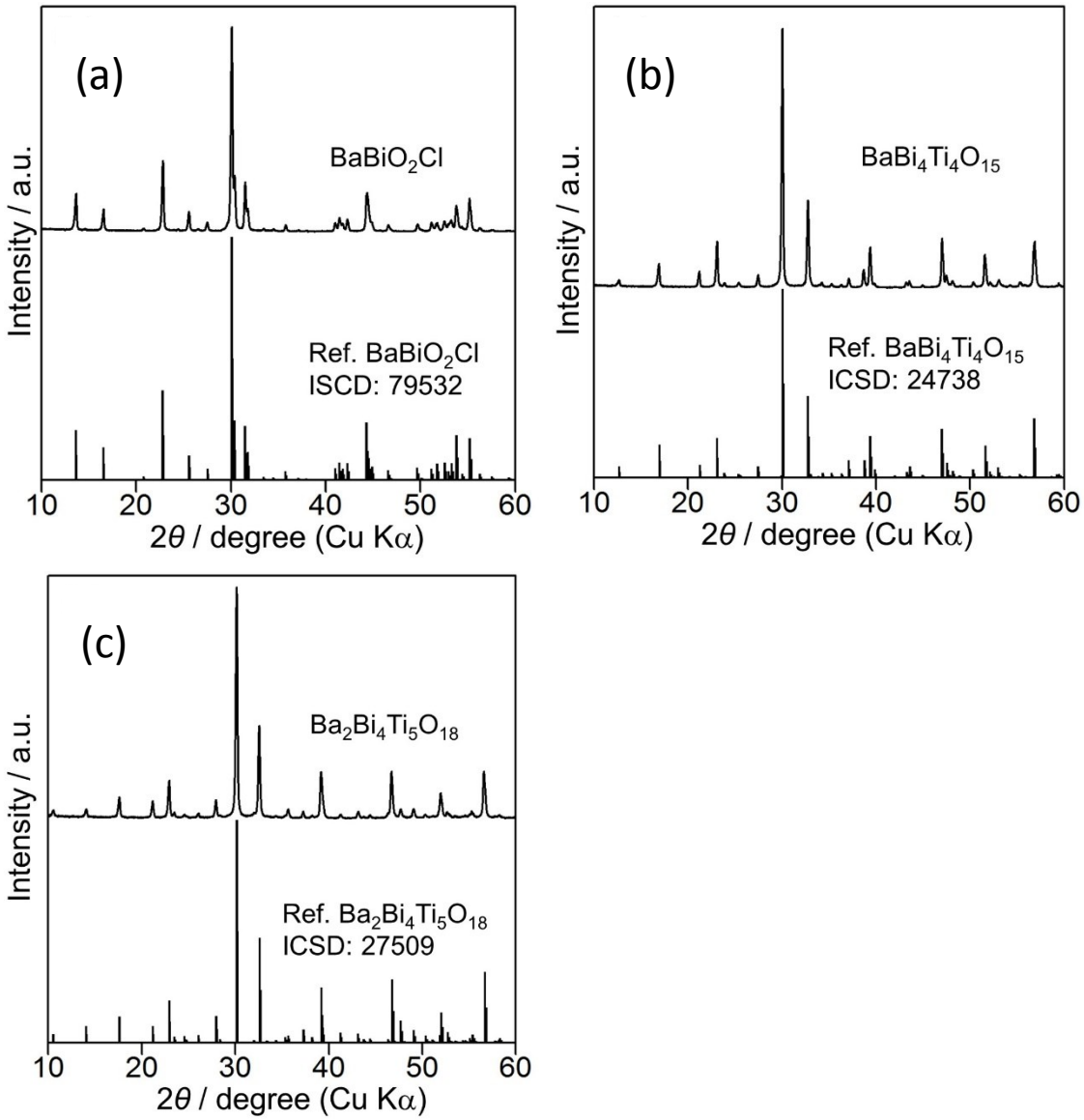

Fig. S3 XRD patterns of (a) $BaBiO_2Cl$, (b) $BaBi_4Ti_4O_{15}$ and (c) $Ba_2Bi_4Ti_5O_{18}$.

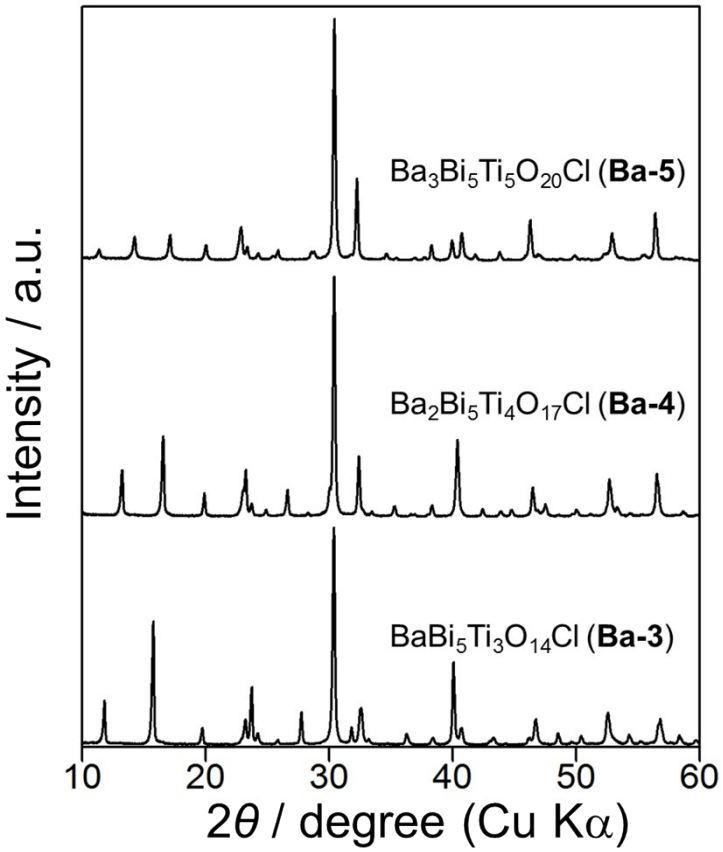

Fig. S4 Laboratory XRD patterns of $BaBi_5Ti_3O_{14}Cl$ (**Ba-3**), $Ba_2Bi_5Ti_4O_{17}Cl$ (**Ba-4**) and $Ba_3Bi_5Ti_5O_{20}Cl$ (**Ba-5**).

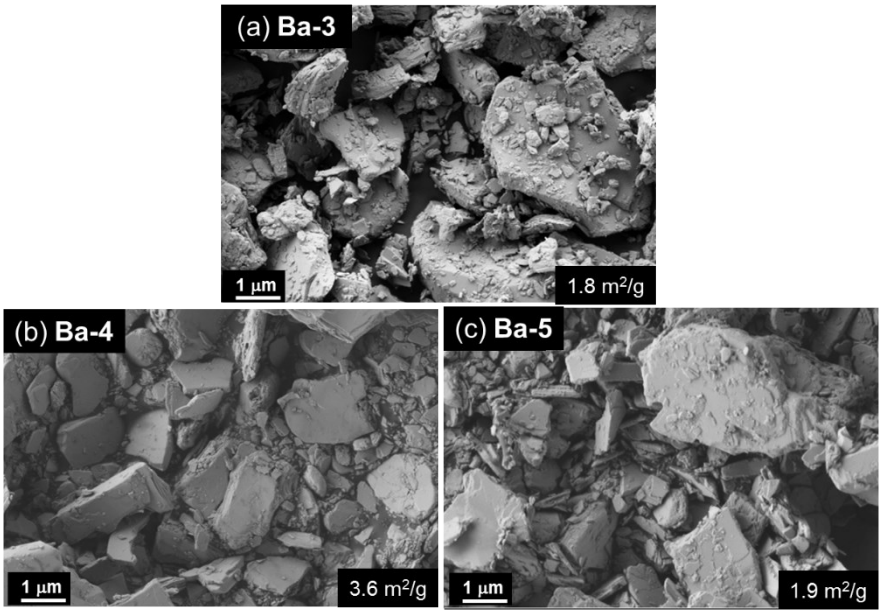

Fig. S5 SEM images of $BaBi_5Ti_3O_{14}Cl$ (**Ba-3**), $Ba_2Bi_5Ti_4O_{17}Cl$ (**Ba-4**) and $Ba_3Bi_5Ti_5O_{20}Cl$ (**Ba-5**) and their specific surface areas.

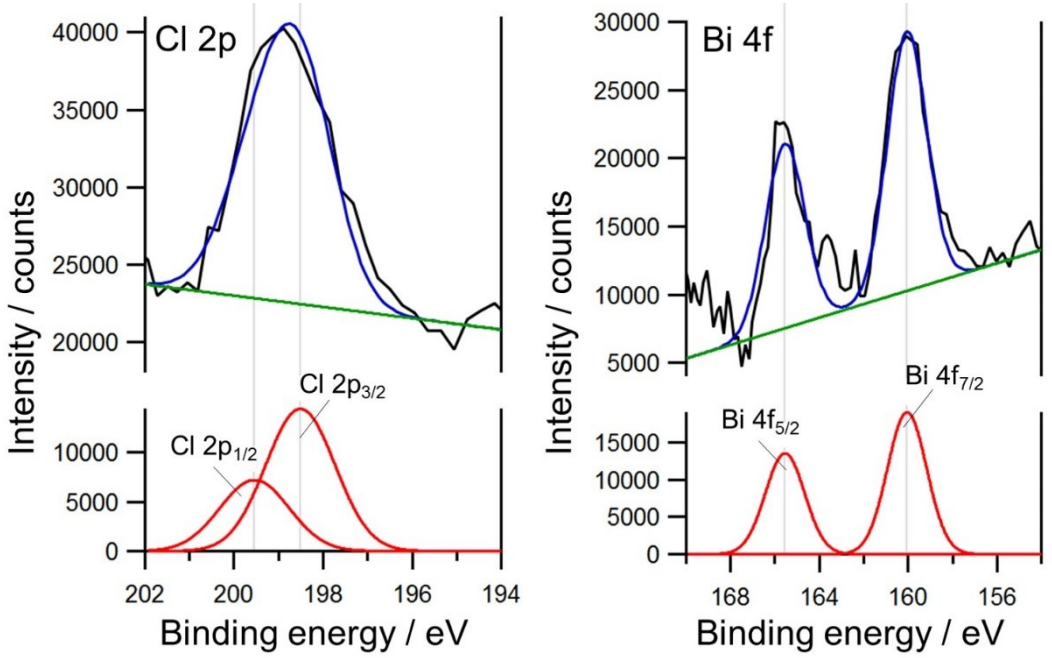

Fig. S6 EUPS spectra of $BaBi_5Ti_3O_{14}Cl$ (**Ba-3**). (left) Cl 2p (Cl $2p_{1/2}$ area: 14038; Cl $2p_{3/2}$ area: 28076; total area: 42114) and (right) Bi 4f (Bi $4f_{5/2}$ area: 29932; Bi $4f_{7/2}$ area: 42096; total area: 72028).

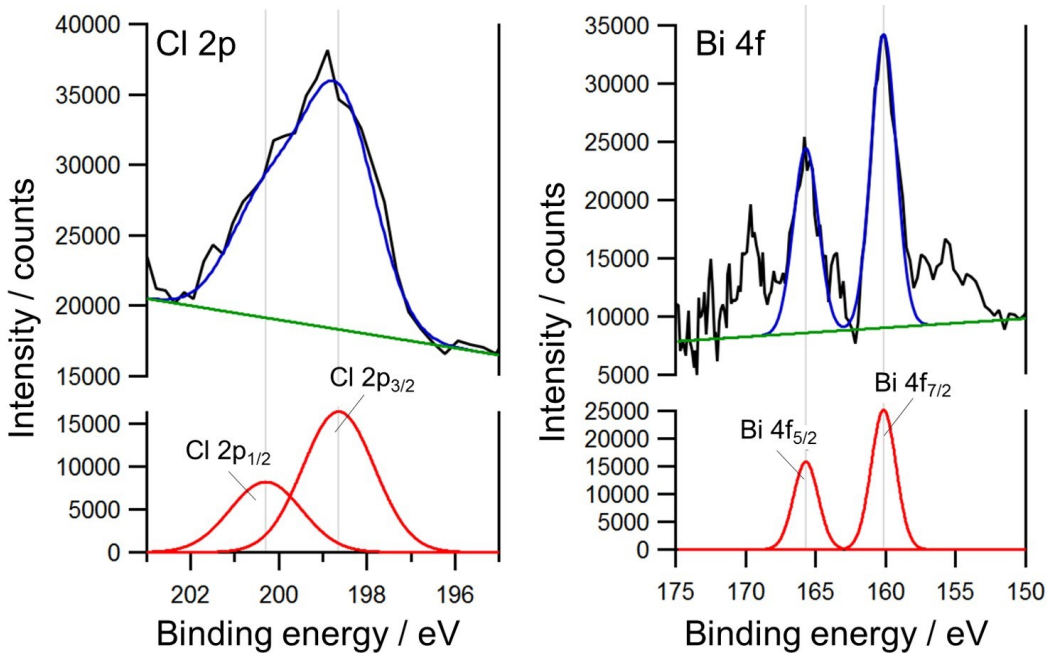

Fig. S7 EUPS spectra of $Ba_2Bi_5Ti_4O_{17}Cl$ (**Ba-4**). (left) Cl 2p (Cl $2p_{1/2}$ area: 16714; Cl $2p_{3/2}$ area: 33428; total area: 50142) and (right) Bi 4f (Bi $4f_{5/2}$ area: 35083; Bi $4f_{7/2}$ area: 55879; total area: 90962).

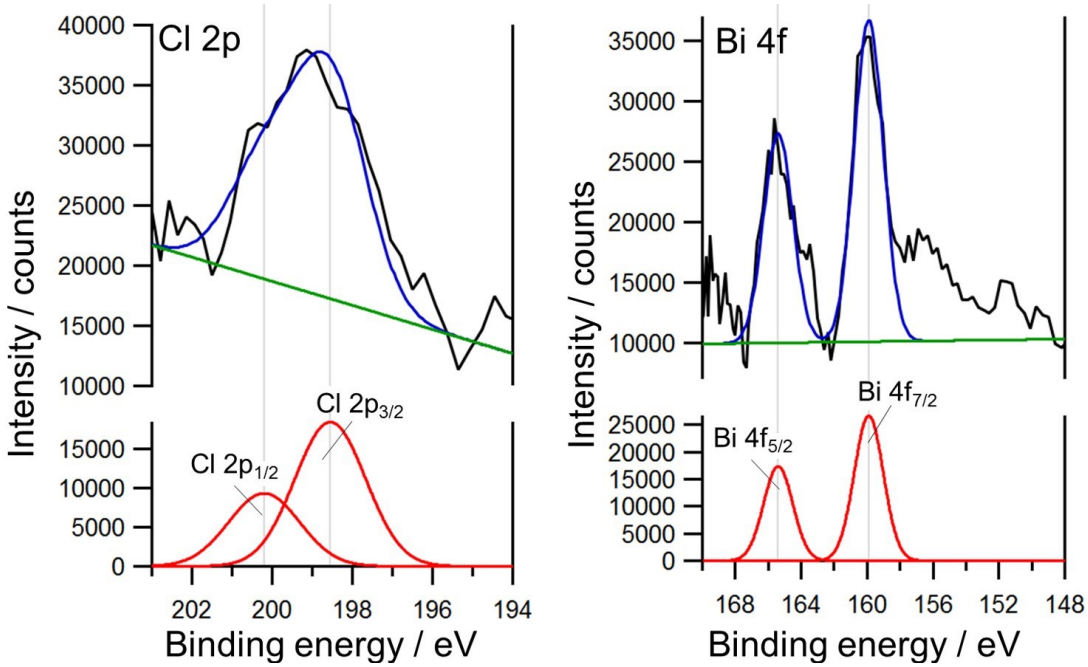

Fig. S8 EUPS spectra of $Ba_3Bi_5Ti_5O_{20}Cl$ (**Ba-5**). (left) Cl 2p (Cl $2p_{1/2}$ area: 20578; Cl $2p_{3/2}$ area: 40659; total area: 61237) and (right) Bi 4f (Bi $4f_{5/2}$ area: 38422; Bi $4f_{7/2}$ area: 58970; total area: 97392).

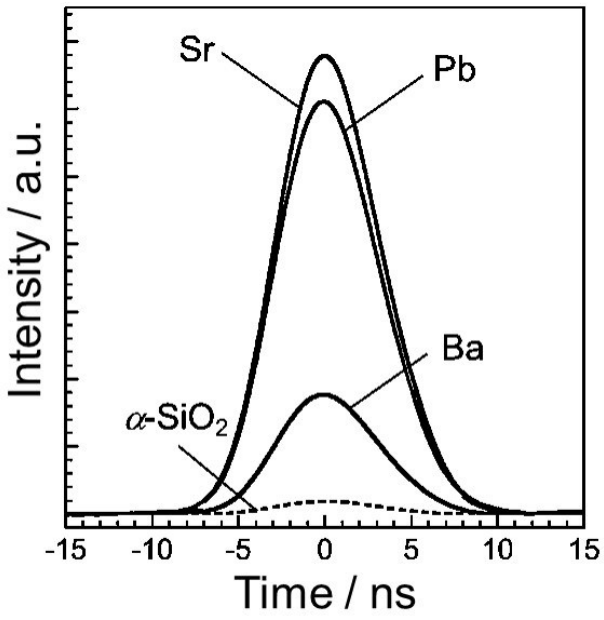

Fig. S9 SHG intensities for $BaBi_5Ti_3O_{14}Cl$ (**Ba-3**). $Bi_5MTi_3O_{14}Cl$ (*M* = Sr, Pb) and α-SiO_2 are references.

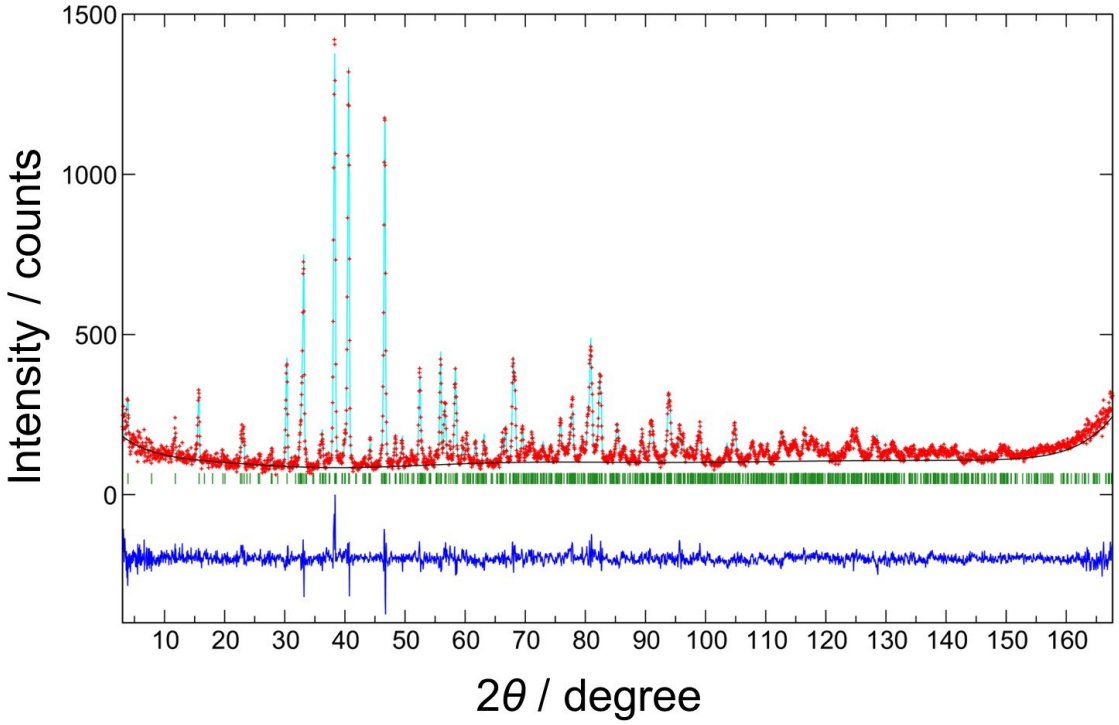

Fig. S10 Final Rietveld plot for $BaBi_5Ti_3O_{14}Cl$ (**Ba-3**) using the NPD pattern collected at room temperature; R_p = 0.0754, R_{wp} = 0.0966, R_B = 0.0713, R_F = 0.0310, χ^2 = 1.171.

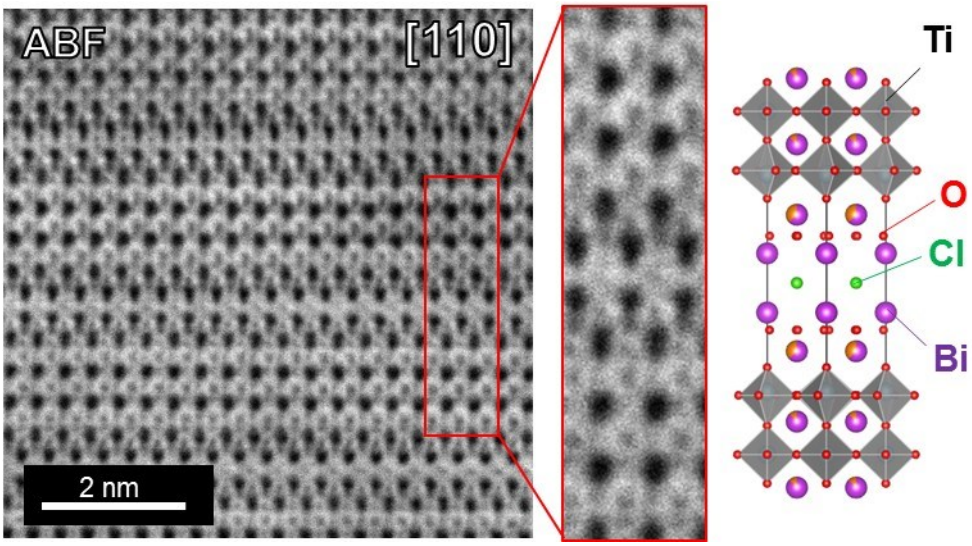

Fig. S11 ABF-STEM images of $BaBi_5Ti_3O_{14}Cl$ (**Ba-3**) in the direction of [110].

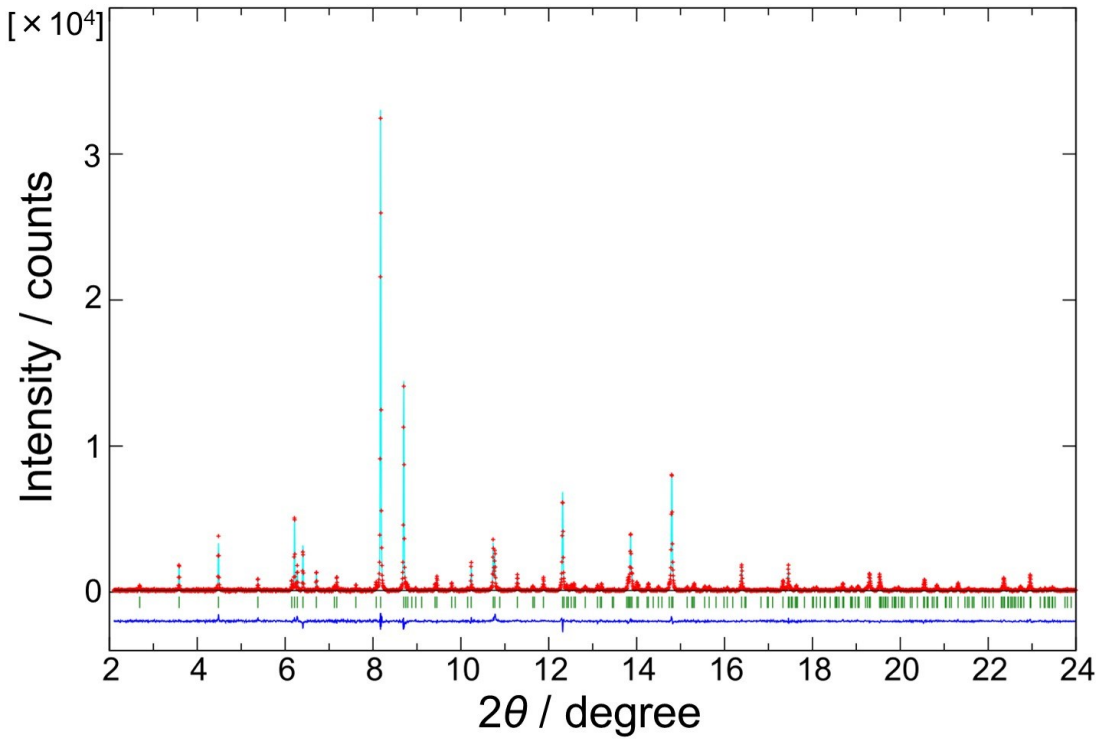

Fig. S12 Final Rietveld plot for $Ba_2Bi_5Ti_4O_{17}Cl$ (**Ba-4**) using the SXRD pattern collected at room temperature; R_p = 0.1184, R_{wp} = 0.1761, R_B = 0.0620, R_F = 0.0526, χ^2 = 2.884.

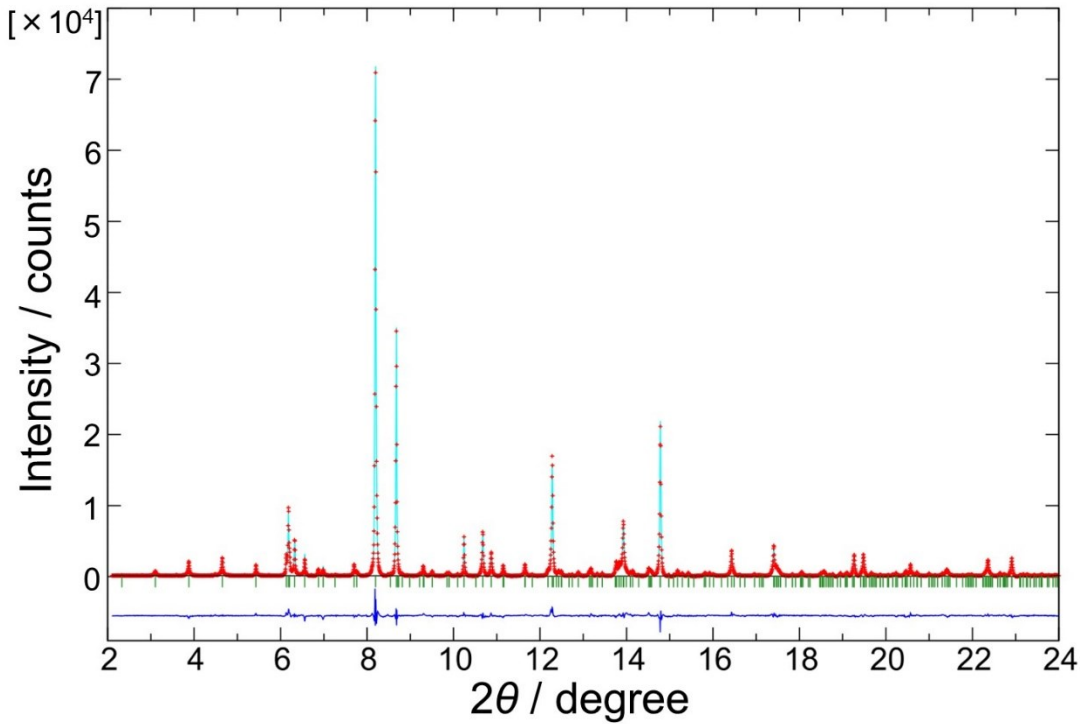

Fig. S13 Final Rietveld plot for $Ba_3Bi_5Ti_5O_{20}Cl$ (**Ba-5**) using the SXRD pattern collected at room temperature; R_p = 0.0944, R_{wp} = 0.1437, R_B = 0.0468, R_F = 0.0365, χ^2 = 3.609.

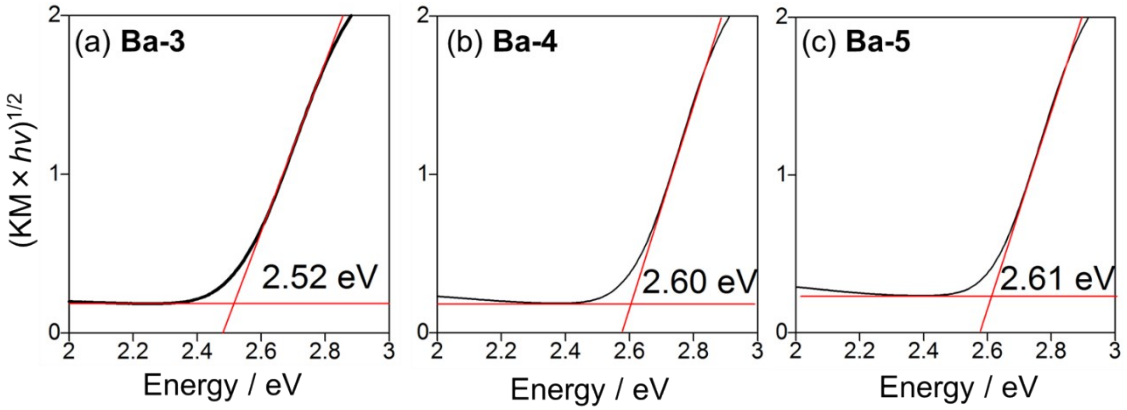

Fig. S14 Tauc plots of (a) $BaBi_5Ti_3O_{14}Cl$ (**Ba-3**), (b) $Ba_2Bi_5Ti_4O_{17}Cl$ (**Ba-4**) and (c) $Ba_3Bi_5Ti_5O_{20}Cl$ (**Ba-5**).

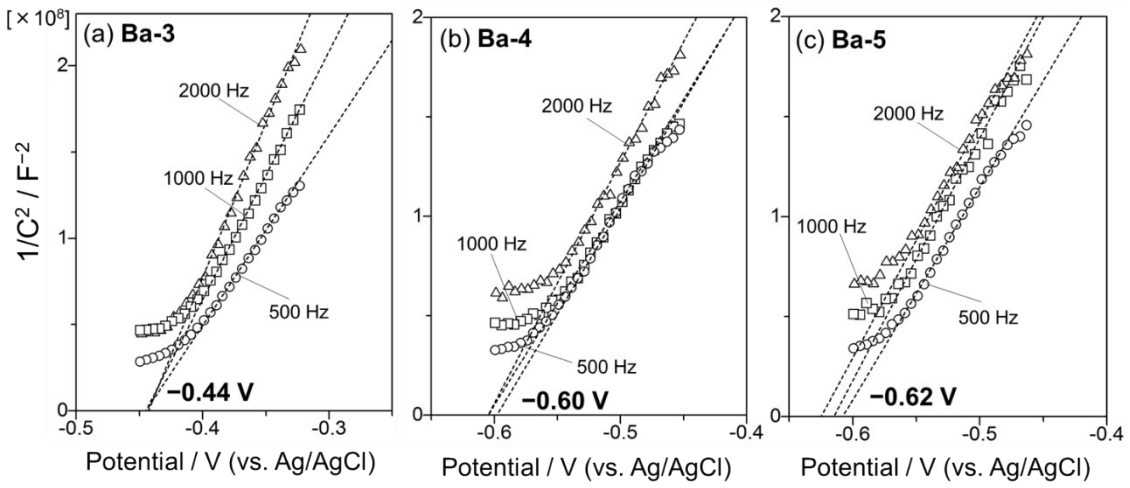

Fig. S15 Mott–Schottky plots of (a) $BaBi_5Ti_3O_{14}Cl$ (**Ba-3**), (b) $Ba_2Bi_5Ti_4O_{17}Cl$ (**Ba-4**) and (c) $Ba_3Bi_5Ti_5O_{20}Cl$ (**Ba-5**) collected in an aqueous Na_2SO_4 solution (0.1 M, pH 2.0, adjusted by 0.5 M H_2SO_4) with the amplitude and frequency were set to 10 mV and 500, 1000, 2000 Hz, respectively.

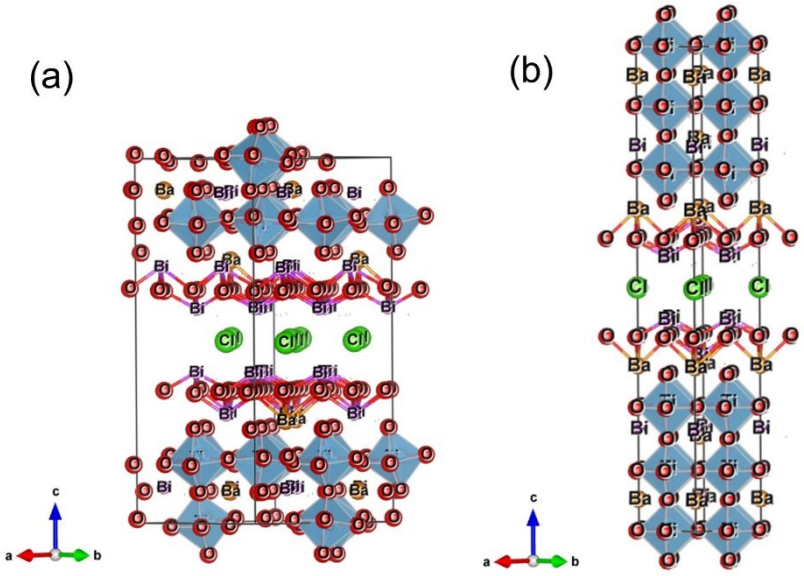

Fig. S16 Structural models employed for the DFT calculation; (a) 192-atom supercell of $BaBi_5Ti_3O_{14}Cl$ (**Ba-3**) and (b) 68-atom supercell of $Ba_3Bi_5Ti_5O_{20}Cl$ (**Ba-5**).

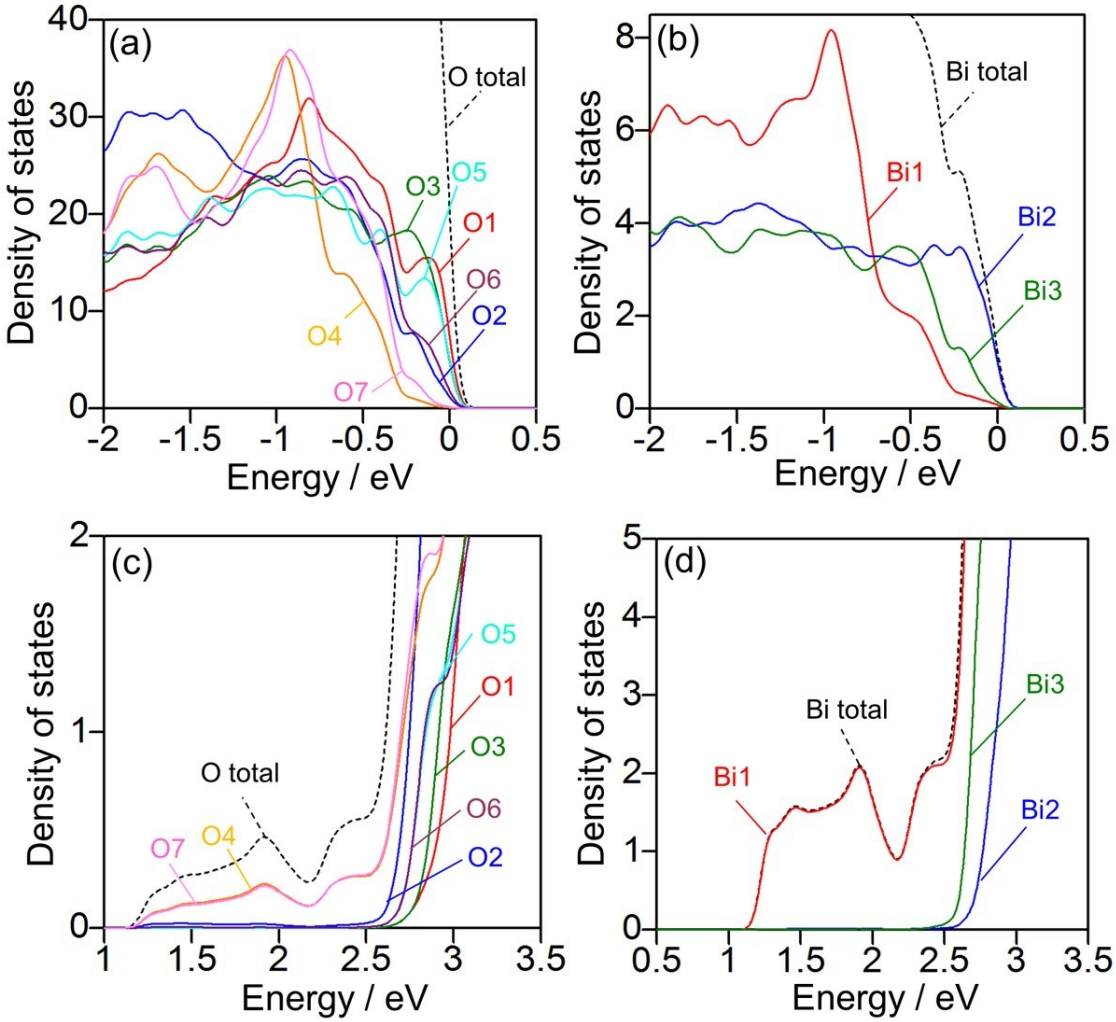

Fig. S17 PDOS around the VBM from (a) each O site and (b) Bi site, and around the CBM from (c) each O site and (d) Bi site in $BaBi_5Ti_3O_{14}Cl$ (**Ba-3**). See Fig. 5 for the detailed labelling.

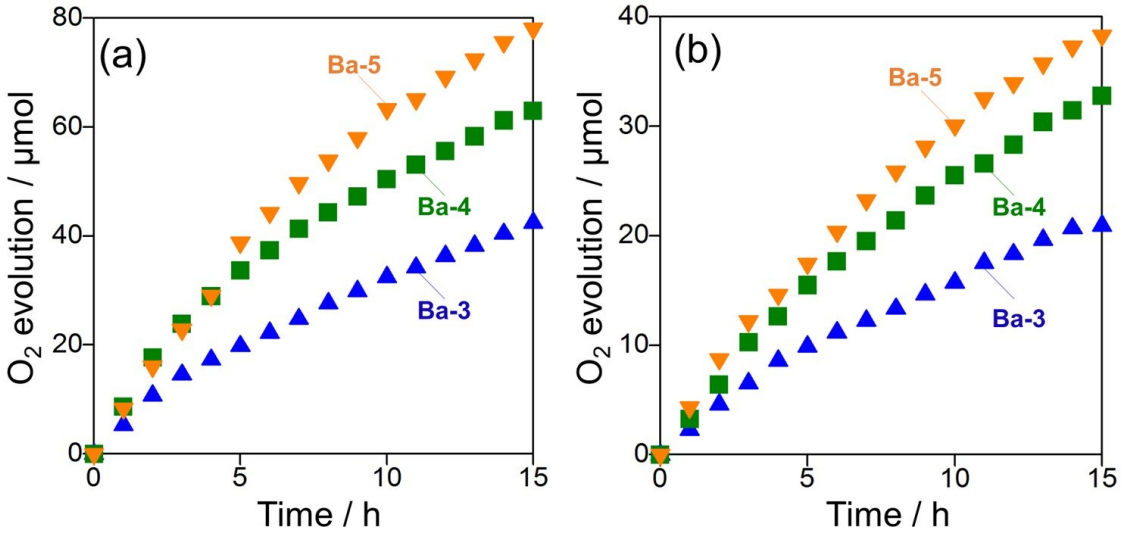

Fig. S18 Time courses of photocatalytic O_2 evolution on 100 mg of $BaBi_5Ti_3O_{14}Cl$ (**Ba-3**), $Ba_2Bi_5Ti_4O_{17}Cl$ (**Ba-4**) and $Ba_3Bi_5Ti_5O_{20}Cl$ (**Ba-5**) photocatalysts under visible light ($400 < \lambda < 800$ nm) in aqueous solutions of (a) $AgNO_3$ (10 mM,120 mL) and (b) $Fe(ClO_4)_3$ (5 mM, 120 mL, pH 2.3, adjusted by $HClO_4$).

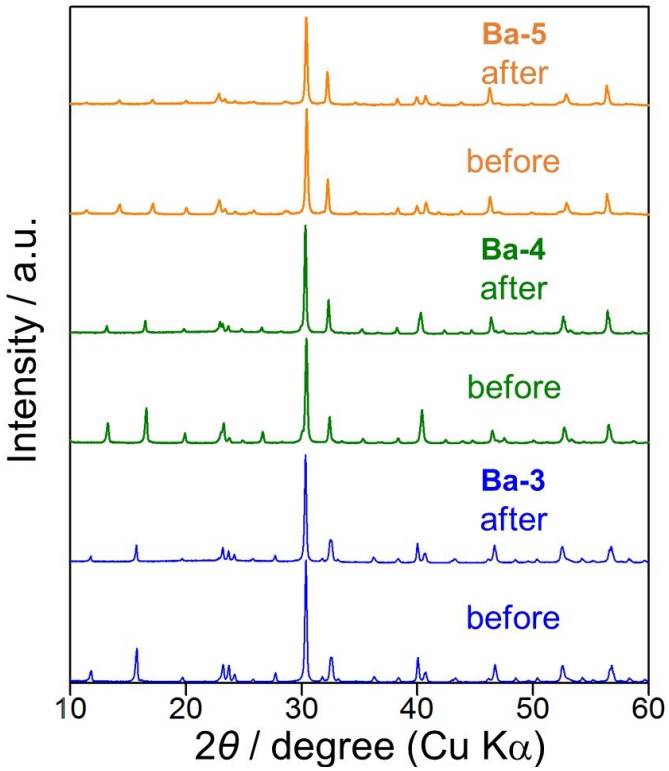

Fig. S19 XRD patterns of $BaBi_5Ti_3O_{14}Cl$ (**Ba-3**), $Ba_2Bi_5Ti_4O_{17}Cl$ (**Ba-4**) and $Ba_3Bi_5Ti_5O_{20}Cl$ (**Ba-5**) before and after photocatalytic O_2 evolution in an $Fe(ClO_4)_3$ aqueous solution under visible light.

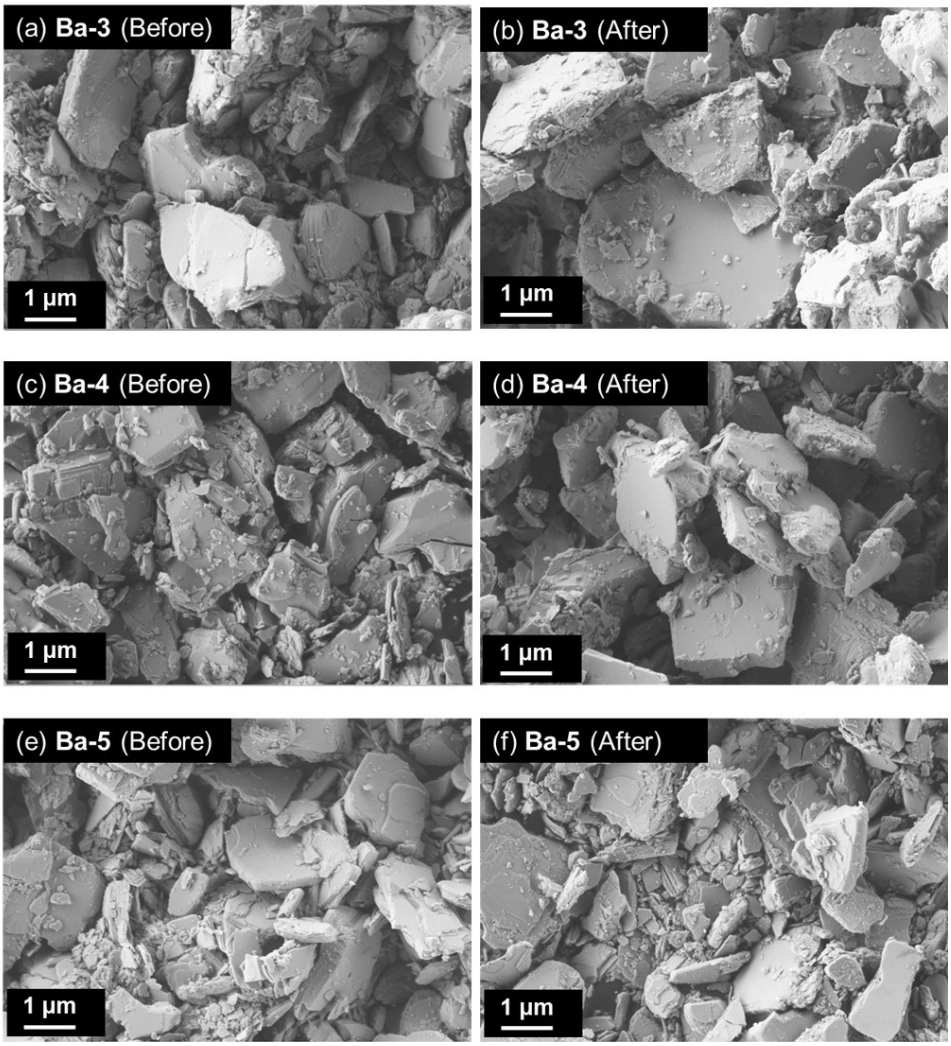

Fig. S20 SEM images of $BaBi_5Ti_3O_{14}Cl$ (**Ba-3**), $Ba_2Bi_5Ti_4O_{17}Cl$ (**Ba-4**) and $Ba_3Bi_5Ti_5O_{20}Cl$ (**Ba-5**) before and after photocatalytic O_2 evolution in an $Fe(ClO_4)_3$ aqueous solution under visible light.

Table S1 Final refined structure parameters for $BaBi_5Ti_3O_{14}Cl$ (**Ba-3**)[a]

Atom	Site	*x*	*y*	*z*	*g*	100*U* / Å²	BVS
Bi/Ba1	4*c*	0.031(3)	-0.000(3)	0.41350(9)	Bi: 1	1.13(5)	3.1[e]
Bi/Ba2	4*c*	0[b]	0.497(3)	0.0956(10)	Bi: 0.874(2) Ba: 0.126(2)	2.56(7)	2.4[e]
Bi/Ba3	4*c*	0.038(14)	0.495(2)	0.3008(11)	Bi: 0.626(2) Ba: 0.374(2)	2.55(7)	2.2[e]
Ti1	2*a*	0.018(8)	0	0	1	0.3(2)[c]	3.9
Ti2	4*c*	0.009(6)	-0.00(11)	0.1843(4)	1	0.3(2)[c]	4.2
Cl1	2*b*	0.026(4)	1/2	1/2	1	1.8(14)	-
O1	4*c*	-0.014(3)	-0.035(3)	0.0896(5)	1	2.54(7)[d]	-
O2	4*c*	0.050(4)	0.023(4)	0.2623(4)	1	2.54(7)[d]	-
O3	4*c*	0.293(3)	0.218(4)	0.004(11)	1	2.54(7)[d]	-
O4	4*c*	0.281(5)	0.245(9)	0.3646(9)	1	2.54(7)[d]	-
O5	4*c*	0.319(4)	0.222(4)	0.1688(8)	1	2.54(7)[d]	-
O6	4*c*	0.775(4)	0.734(6)	0.1773(7)	1	2.54(7)[d]	-
O7	4*c*	0.783(5)	0.744(8)	0.363(10)	1	2.54(7)[d]	-

[a]Space group *P*2*an* (#30), orthorhombic, a = 5.50525(6) Å, b = 5.48057(5) Å, c = 22.4870(2) Å, V = 678.49(12) Å^3. [b]Fixed to define origin of polar axis. [c]Constrained to be equivalent to Ti1. [d]Constrained to be equivalent to O1. [e]Calculated by using bond valence parameter of Bi^{3+}.

Table S2 Bond lengths of $BaBi_5Ti_3O_{14}Cl$ (**Ba-3**)

Bond	Bond length / Å
Ti1–O1	2.032(13) × 2
Ti1–O3	1.93(4)×2, 1.98(4) × 2
Ti2–O1	2.140(16)
Ti2–O2	1.770(14)
Ti2–O5	1.89(6), 2.13(5)
Ti2–O6	1.95(6), 1.95(6)
Bi1–O4	2.22(4), 2.25(4)
Bi1–O7	2.23(1), 2.26(1)
Bi1–Cl1	3.349(17), 3.360(14), 3.361(14), 3.392(18)
Bi2–O1	2.57(3), 2.685(18), 2.842(18), 2.92(3)
Bi2–O3	2.64(3), 2.78(3), 3.04(3), 3.17(3)
Bi2–O5	2.27(3), 2.84(3)
Bi2–O6	2.57(3), 2.84(3)
Bi3–O2	2.82(3), 2.847(14), 2.902(14), 2.95(3)
Bi3–O4	2.39(4), 2.41(4)
Bi3–O7	2.42(4), 2.41(4)

Table S3 Final refined structure parameters for $Ba_2Bi_5Ti_4O_{17}Cl$ (**Ba-4**)[a]

Atom	Site	*x*	*y*	*z*	*g*	100*U* / Å²	BVS
Bi/Ba1	2*h*	1/2	1/2	0.4267(12)	Bi: 1	1.01(6)	3.5[c]
Bi/Ba2	2*g*	0	0	Bi2: 0.3385(2) Ba2: 0.3133(6)	Bi: 0.670(3) Ba: 0.330(3)	1.7(10)	2.1[c]
Bi/Ba3	2*g*	0	0	Bi3: 0.1669(3) Ba3: 0.1505(5)	Bi: 0.574(3) Ba: 0.426(3)	2.4(11)	2.5[c]
Bi/Ba4	1*a*	0	0	0	Bi: 0.512(3) Ba: 0.488(3)	3.5(2)	2.1[c]
Ti1	2*h*	1/2	1/2	0.2364(5)	1	1.1(3)	4.2
Ti2	2*h*	1/2	1/2	0.0769(6)	1	0.9(3)	3.7
Cl1	1*b*	0	0	1/2	1	2.4(7)	-
O1	4*i*	0	1/2	0.391(12)	1	1.2(3)[b]	-
O2	2*h*	1/2	1/2	0.298(2)	1	1.2(3)[b]	-
O3	4*i*	0	1/2	0.220(11)	1	1.2(3)[b]	-
O4	2*h*	1/2	1/2	0.153(2)	1	1.2(3)[b]	-
O5	4*i*	0	1/2	0.070(11)	1	1.2(3)[b]	-
O6	1*c*	1/2	1/2	0	1	1.2(3)[b]	-

[a]Space group *P*4/*mmm* (#123), tetragonal, $a = b = 3.91036(4)$ Å, $c = 26.8125(4)$ Å, $V = 409.988(9)$ Å^3. [b]Constrained to be equivalent to O1. [c]Calculated by using bond valence parameter of Bi^{3+}.

Table S4 Final refined structure parameters for $Ba_3Bi_5Ti_5O_{20}Cl$ (**Ba-5**)[a]

Atom	Site	*x*	*y*	*z*	*g*	100*U* / Å²	BVS
Bi/Ba1	2*h*	1/2	1/2	0.43608(7)	Bi: 1	2.15(6)	3.2[d]
Bi/Ba2	2*g*	0	0	Bi2: 0.3611(11) Ba2: 0.3413(3)	Bi: 0.573(4) Ba: 0.427(4)	2.20(10)	2.4[d]
Bi/Ba3	2*g*	0	0	Bi3: 0.2042(2) Ba3: 0.2167(3)	Bi: 0.489(4) Ba: 0.511(4)	2.03(9)	2.0[d]
Bi/Ba4	2*g*	0	0	Bi4: 0.0629(2) Ba4: 0.0753(2)	Bi: 0.438(4) Ba: 0.562(4)	2.96(9)	2.0[d]
Ti1	2*h*	1/2	1/2	0.2725(3)	1	0.6(2)[b]	4.4
Ti2	2*h*	1/2	1/2	0.1343(3)	1	0.6(2)[b]	4.1
Ti3	1*c*	1/2	1/2	0	1	0.6(2)[b]	4.3
Cl1	1*b*	0	0	1/2	1	1.8(5)	-
O1	4*i*	0	1/2	0.4029(7)	1	0.8(2)[c]	-
O2	2*h*	1/2	1/2	0.323(10)	1	0.8(2)[c]	-
O3	4*i*	0	1/2	0.2566(7)	1	0.8(2)[c]	-
O4	2*h*	1/2	1/2	0.191(11)	1	0.8(2)[c]	-
O5	4*i*	0	1/2	0.1261(7)	1	0.8(2)[c]	-
O6	2*h*	1/2	1/2	0.061(11)	1	0.8(2)[c]	-
O7	2*f*	0	1/2	0	1	0.8(2)[c]	-

[a]Space group *P*4/*mmm* (#123), tetragonal, $a = b = 3.92036(4)$ Å, $c = 30.9881(7)$ Å, $V = 476.26(12)$ Å^3. [b]Constrained to be equivalent to Ti1. [c]Constrained to be equivalent to O1. [d]Calculated by using bond valence parameter of Bi^{3+}.

Table S5 Bond lengths of $Ba_2Bi_5Ti_4O_{17}Cl$ (**Ba-4**) and $Ba_3Bi_5Ti_5O_{20}Cl$ (**Ba-5**)

Bond	Bond length / Å	
	Ba-4	**Ba-5**
Ti1–O2	1.66(5)	1.57(4)
Ti1–O3	2.004(8) × 4	2.001(6) × 4
Ti1–O4	2.24(5)	2.53(4)
Ti2–O4	2.04(5)	1.76(4)
Ti2–O5	1.963(4) × 4	1.977(3)
Ti2–O6	2.061(16)	2.26(4)
Ti3–O6	-	1.90(4)
Ti3–O7	-	1.960
Bi1–Cl1	3.3920(19) × 4	3.4071(13) × 4
Bi1–O1	2.176(15) × 4	2.214(10) × 4
Bi2–O1	2.411(19) × 4	2.348(12) × 4
Ba2–O1	2.86(3) × 4	2.736(16) × 4
Bi2–O2	2.966(16) × 4	3.011(13) × 4
Ba2–O2	2.794(7) × 4	2.828(7) × 4
Bi3–O3	2.418(18) × 4	2.546(14) × 4
Ba3–O3	2.70(3) × 4	2.317(12) × 4
Bi3–O4	2.791(6) × 4	2.802(5) × 4
Ba3–O4	2.7657(10) × 4	2.885(10) × 4
Bi3–O5	3.25(3) × 4	3.113(17) × 4
Ba3–O5	2.91(3) × 4	3.424(18) × 4
Bi4–O5	2.72(3) × 4	2.771(15) × 4
Bi4–O6	2.76504(3) × 4	2.7726(6) × 4
Bi4–O7	-	2.765(4) × 4
Bi4–O5	-	2.516(14) × 4
Bi4–O6	-	2.806(6) × 4
Bi4–O7	-	3.046(6) × 4

Table S6 Comparison between calculated and experimental band gaps of **Ba-3** and **Ba-5**

Material	Band gap / eV	
	DFT (GGA-PBE)	**Experimental**
Ba-3	1.20 (−52.4%)[a]	2.52
Ba-5	0.55 (−78.9%)[a]	2.61

[a]Error to the experimental value

Table S7 Comparison between calculated and experimental lattice parameters of **Ba-3** and **Ba-5**

Ba-3	***a* / Å**	***b* / Å**	***c* / Å**
DFT	11.27 (+2.4%)[a]	11.17 (+1.9%)[a]	22.66 (+0.8%)[a]
Experimental	11.01	10.96	22.49

Ba-5	***a* / Å**	***b* / Å**	***c* / Å**
DFT	5.61 (1.3%)[a]	5.61 (1.3%)[a]	31.52 (1.7%)[a]
Experimental	5.54	5.54	30.99

[a]Error to the experimental value